Supplement of Geosci. Model Dev., 14, 4117–4141, 2021
https://doi.org/10.5194/gmd-14-4117-2021-supplement
© Author(s) 2021. CC BY 4.0 License.

Geoscientific Model Development
Open Access
EGU

Supplement of

CM2Mc-LPJmL v1.0: biophysical coupling of a process-based dynamic vegetation model with managed land to a general circulation model

Markus Drüke et al.

Correspondence to: Markus Drüke (drueke@pik-potsdam.de)

The copyright of individual parts of the supplement might differ from the article licence.

S1 Seasonal maps for simulated temperature and precipitation

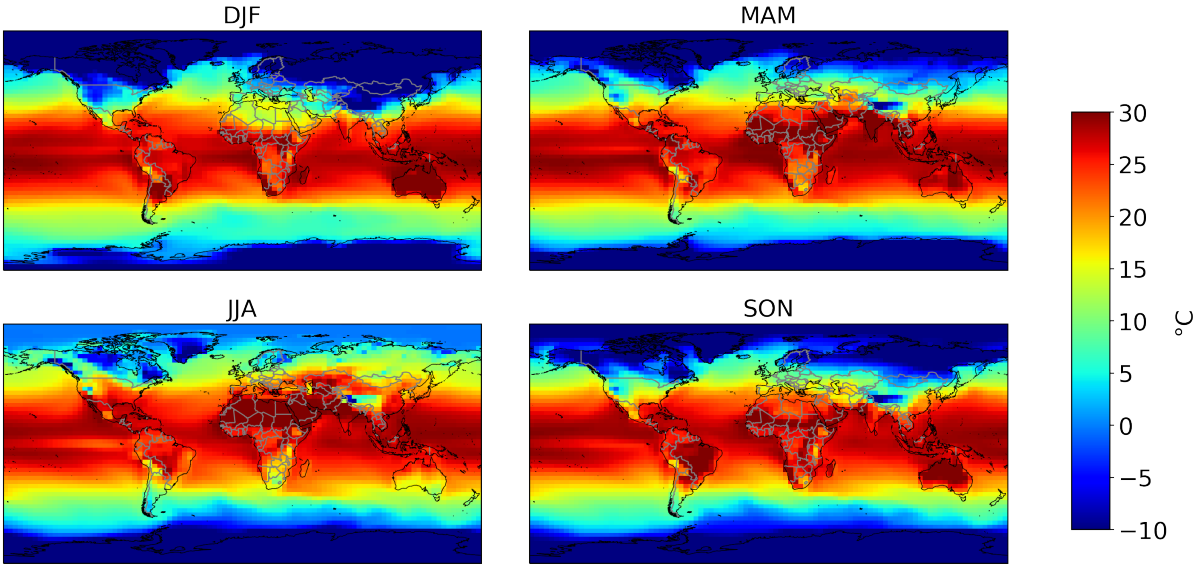

Figure S1. Global mean surface temperature simulated by CM2Mc-LPJmL (TR) for the different seasons (DJF: December-January-February, MAM: March-April-May, JJA: June-July-August, SON: September-October-November), averaged over the period 1994-2003

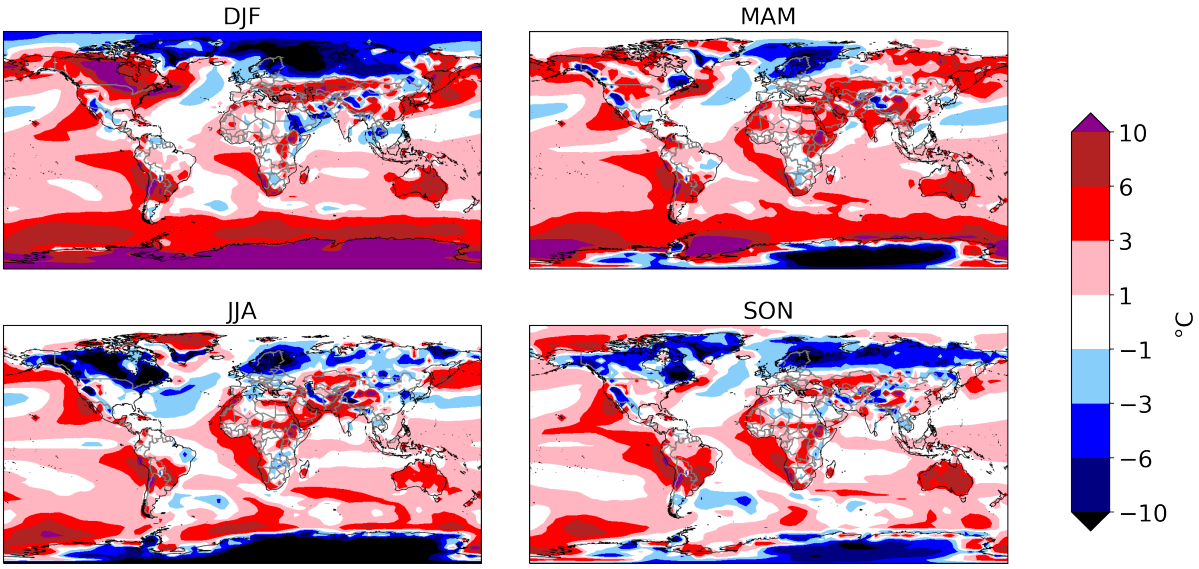

Figure S2. Global surface temperature difference between CM2Mc-LPJmL (TR) and ERA5 data for the different seasons (for abbreviations, see Figure S1) averaged over the period 1994-2003

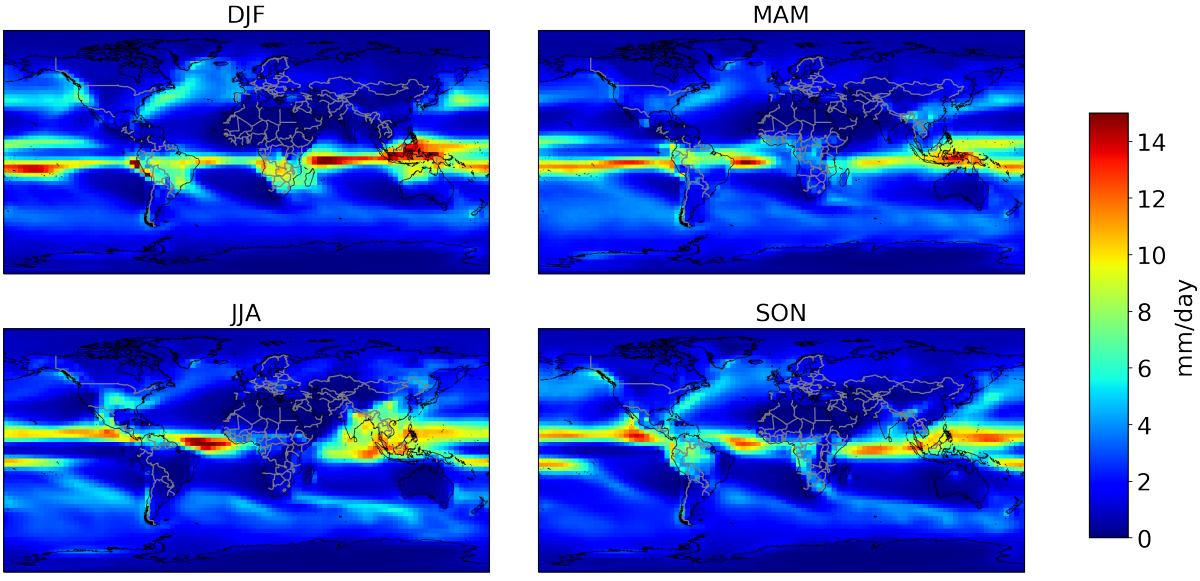

Figure S3. Global mean precipitation modeled by CM2Mc-LPJmL (TR) for the different seasons summed and averaged over the period 1979-2003.

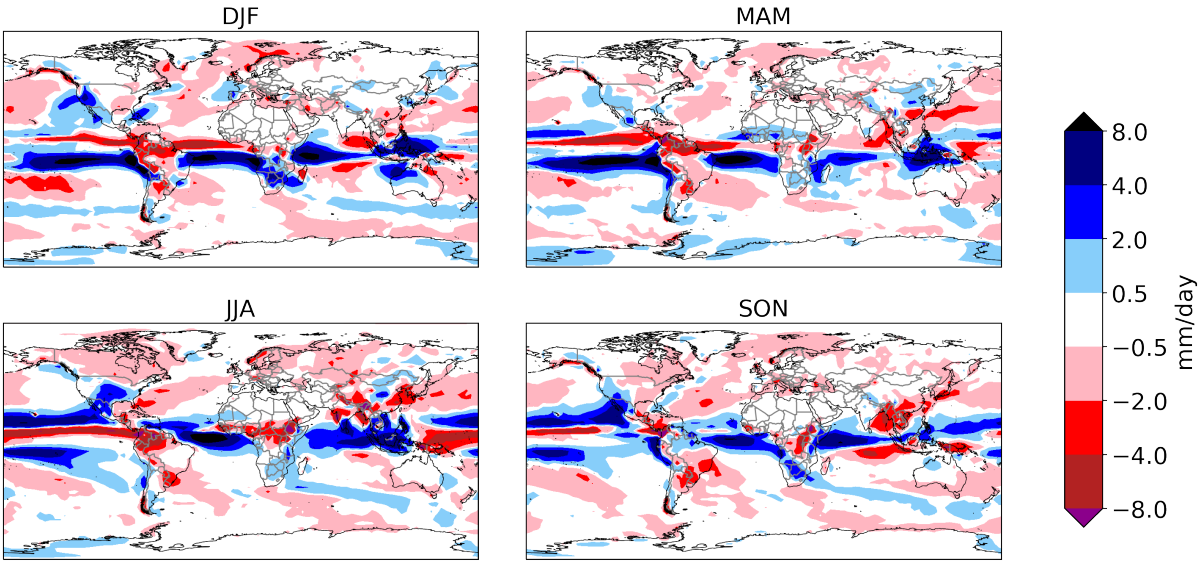

Figure S4. Global precipitation difference between CM2Mc-LPJmL (TR) and ERA5 data for the different seasons ?? over the period 1979-2003.

S2 Climate change impact

In the comparison of the surface temperature of the PNV and the piControl experiments, the very northern and very southern latitudes show a more extreme warming behaviour than lower latitudes (Fig. S5a). The ocean buffers the temperature increase much more than the land and mostly shows a temperature increase by mostly only 0.4-8°C compared to mostly 0.8-1.2°C on the land. The difference in precipitation between both model versions show a more diverse behaviour (Fig. S5b). For example in northern Brazil precipitation is decreasing, while it is increasing in southern Brazil. The patterns over the Pacific indicate a slight shift of the ITCZ. Current climate change and the fertilization effect due to increasing atmospheric CO_2 concentration lead to a global increase of above-ground biomass (Fig. S5d). Especially in the tropical savanna areas this effect is very pronounced with an increase around 4 $kgCm^{-2}$. Only in a few regions (e.g. parts of north America or Scandinavia) the vegetation is slightly decreasing.

After evaluating the historic climate sensitivity by using the PNV version without land use, it is also interesting to compare the response of the Earth System to historic climate change as well as land use change. The climate sensitivity with The PNV experiment is a bit lower compared to GISTEMP evaluation data (S5c). The PNV sensitivity is also a bit worse compared to the TR experiment (Fig. 4).

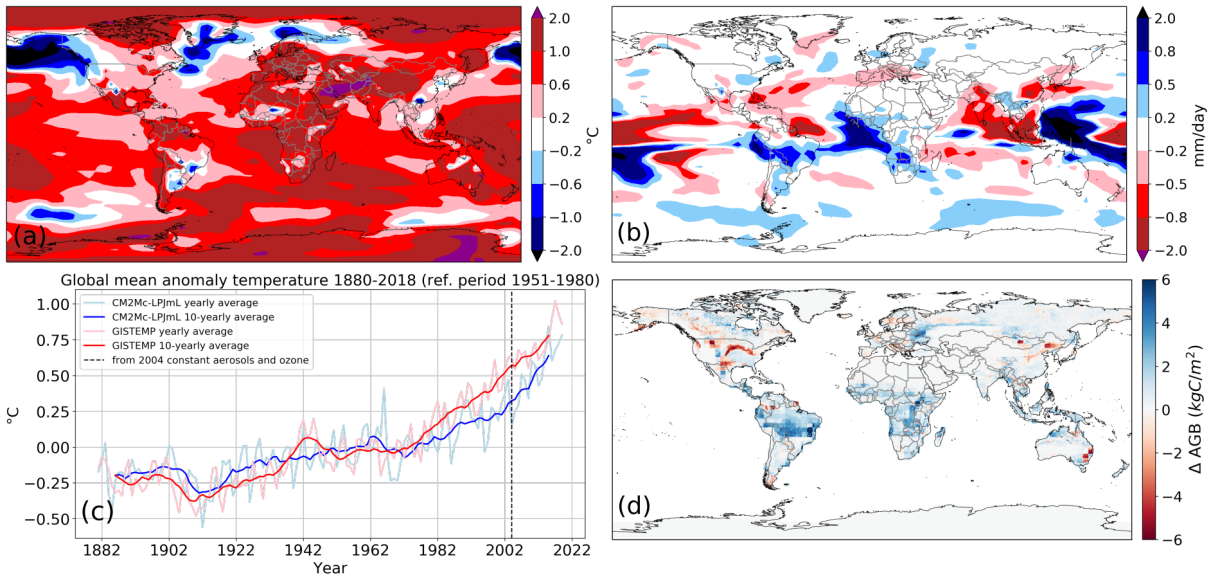

Figure S5. (a) Global temperature difference between the last 10 years of the piControl experiment and the PNV experiment with CM2Mc-LPJmL from 2006-2015. (b) Global precipitation difference between the last 10 years of the pi-Control and the PNV experiments with CM2Mc-LPJmL from 2006-2015. (c) Yearly and decadal global mean anomaly temperature of the PNV experiment of CM2Mc-LPJmL and GISTEMP evaluation data from 1880-2018 to the reference period 1951-1980. (d) Global above-ground biomass difference between the last 10 years of the pi-Control and the PNV experiments with CM2Mc-LPJmL from 2006-2015

S3 Comparison with CM2Mc-LaD

Comparing the results of CM2Mc-LPJmL with the original model CM2Mc including LaD (as in Galbraith et al., 2011), shows similar biases in relation to ERA5 for both model versions. Most prominently, both model versions show the large cold bias in the northern Eurasia and the large hot bias in the southern ocean (Fig. S6a and S6c). CM2Mc-LPJmL shows generally a bit larger biases, resulting in a global average surface temperature of 14.96°C and an NME of 0.16, compared to 14.73°C and an NME of 0.12 of CM2Mc-LaD. ERA5 has a global average surface temperature in the period 1994-2003 of 14.3°C. Hence both CM2Mc versions are much warmer, even when comparing pre-industrial conditions against modern climate data from ERA5. The precipitation bias of CM2Mc-LPJmL and CM2Mc-LaD is even more similar than the temperature bias S6b and S6d). None of the models captures precisely the geographic position of the ITCZ especially over the Pacific. While precipitation close to the equator is underestimated, it is overestimated north and south of it. Both models also show a large dry bias in northern South America. The global average precipitation is quite similar in CM2Mc-LPJmL with 2.86mm/day compared to CM2Mc-LaD with 2.80mm/day. The precipitation in CM2Mc-LPJmL has also a slightly increased NME with 0.51 compared to 0.48 for CM2Mc-LaD.

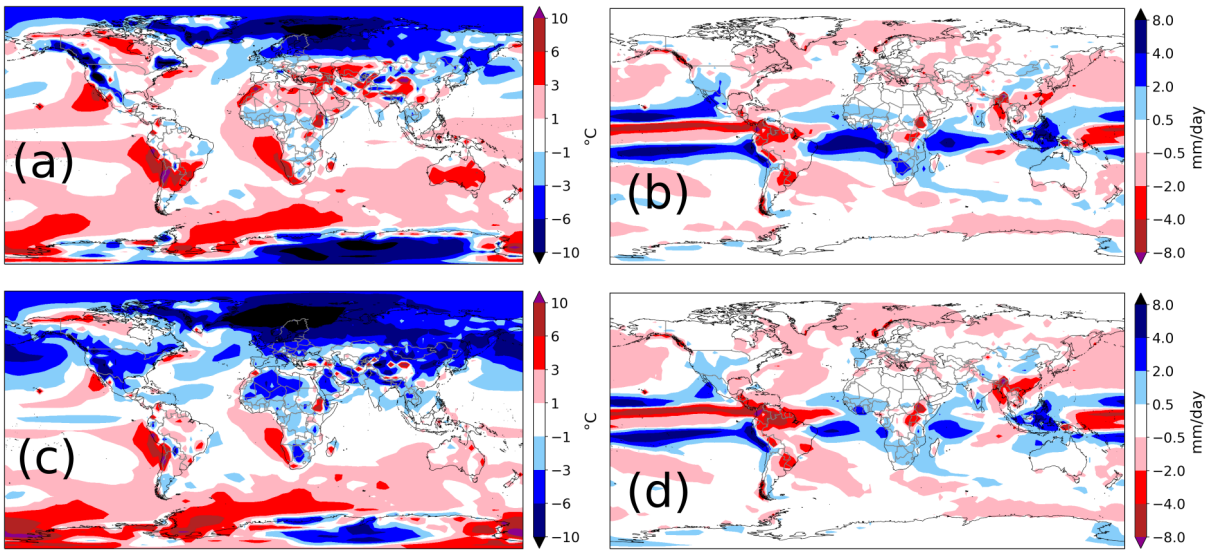

Figure S6. (a) Surface air temperature anomalies between CM2Mc-LPJmL (piControl, last 10 years) and ERA5 data over the period 1994-2003 (b) Global precipitation anomalies between CM2Mc-LPJmL (piControl, last 10 years) and ERA5 data over the period 1994-2003. (c) Surface air temperature anomalies between CM2Mc-LaD (piControl, last 10 years) and ERA5 data over the period 1994-2003 (d) Global precipitation anomalies between CM2Mc-LPJmL (piControl, last 10 years) and ERA5 data over the period 1994-2003

S4 Comparison with CMIP5

We have used data from the fifth phase of the Coupled Model Intercomparison Project (CMIP5) (Taylor et al., 2012) for the historical period to compare simulated carbon fluxes and pools of CM2Mc-LPJmL against state-of-the-art Earth System Model (ESM) results. Our results lie very well in the range of estimations from the provided ESMs, except the soil carbon estimation in the northern latitudes are much higher in CM2Mc-LPJmL (Fig. S7. This is caused by the fact that CM2Mc-LPJmL represents permafrost dynamics and vertical soil carbon distribution, which is in many ESMs missing and thus only a small amount of models are including the high capability of permafrost soils to accumulate carbon (Tamocai et al., 2009). Additionally, we show that our results are within a reasonable range of observations in most latitudes for gross primary production (GPP) and soil and vegetation carbon. (Jung et al., 2011; Carvalhais et al., 2014).

Table S1. Overview of the climate model groups and the available output for each model.

model	VegC	SoilC	LitC	NPP	GPP
BCC-CSM1-1	x	x	x	x	x
BCC-CSM1-1.M	x	x	x	x	x
BNU-ESM	x	x	x	x	x
CESM1-BGC	x	x	x	x	x
CMCC-CESM	x	x	x	x	x
IPSL-CM5A-LR	x	x	x	x	x
IPSL-CM5A-MR	x	x	x	x	x
IPSL-CM5B-LR	x	x	x	x	x
MIROC-ESM	x	x	x	x	x
MIROC-ESM-CHEM	x	x	x	x	x
MPI-ESM-LR	x	x	x	x	x
MPI-ESM-MR	x	x		x	x
MPI-ESM-P				x	x
NorESM1-M				x	x
NorESM1-ME				x	x

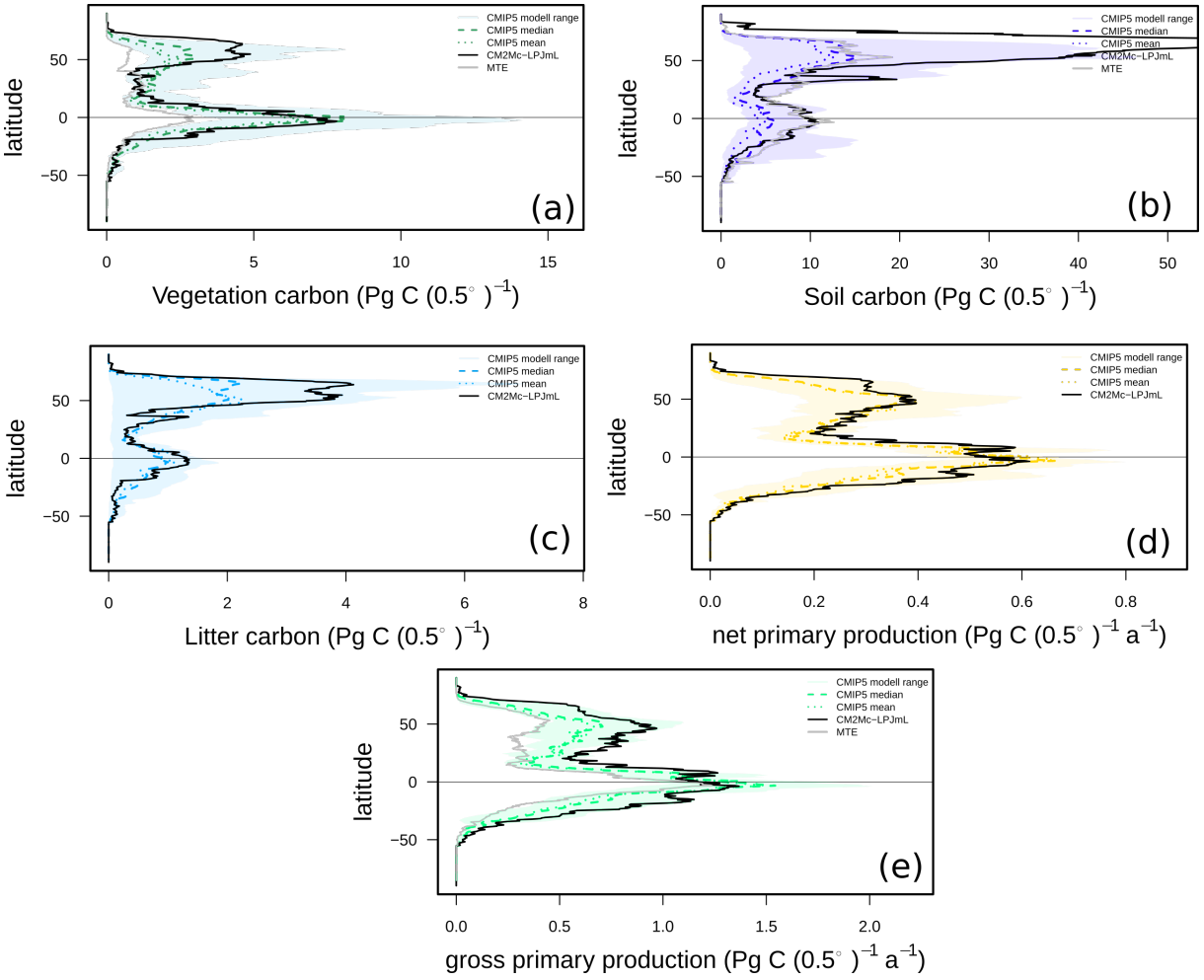

Figure S7. Latitudinal means of CM2Mc-LPJmL results (TR experiment, 2008-2018) compared to CMIP5 results: (a) Vegetation carbon, (b) soil carbon, (c) litter carbon, (d) net primary production, (e) gross primary production. The CM2Mc-LPJmL results are mostly within the range of CMIP5 models. An exception is soil carbon in the northern latitudes, where CM2Mc-LPJmL simulation results are larger than all CMIP5 models.

S5 Carbon stocks in the biosphere

The carbon stocks of the biosphere for the 1000 years of the piControl run show a strong increase until the system stabilizes after ca. 700 years (Fig. S8). The long stabilizing period is due to slow soil processes (e.g. permafrost). There is a difference of ca. 1400 PgC from the start of the coupled run to the value at 700 years, which is due to different climate and processes in the coupled model compared to the stand alone spinup.

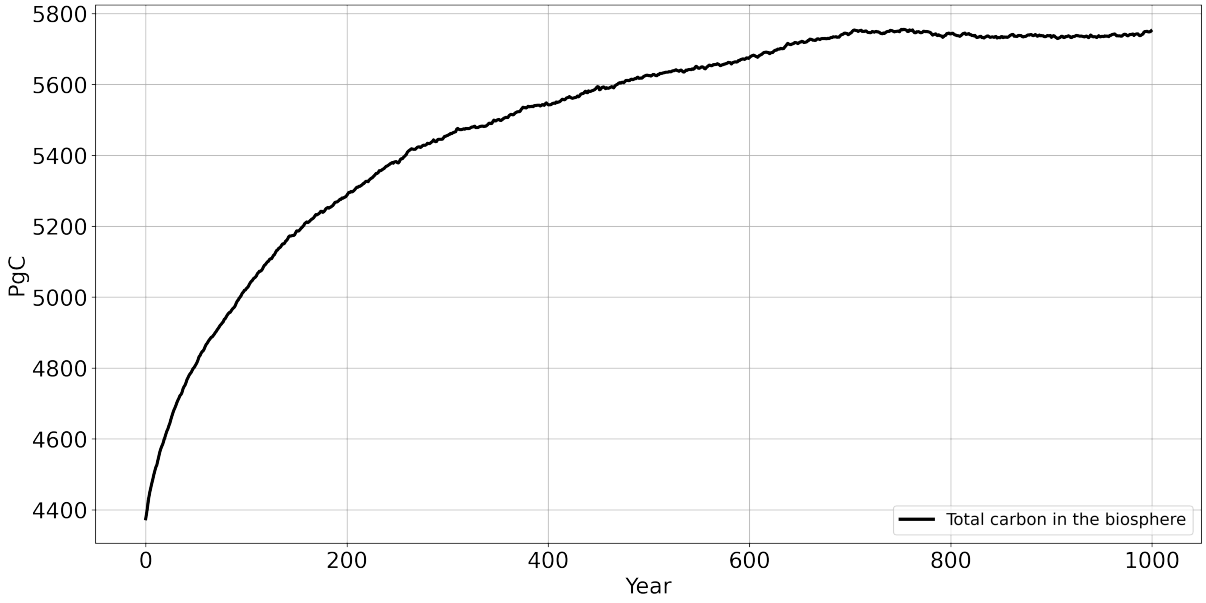

Figure S8. Total carbon in the biosphere (vegetation, litter, soil) for the piControl run.

References

Carvalhais, N., Forkel, M., Khomik, M., Bellarby, J., Jung, M., Migliavacca, M., Mu, M., Saatchi, S., Santoro, M., Thurner, M., Weber, U., Ahrens, B., Beer, C., Cescatti, A., Randerson, J. T., and Reichstein, M.: Global covariation of carbon turnover times with climate in terrestrial ecosystems, Nature, 514, 213–217, https://doi.org/10.1038/nature13731, 2014.

Galbraith, E. D., Kwon, E. Y., Gnanadesikan, A., Rodgers, K. B., Griffies, S. M., Bianchi, D., Sarmiento, J. L., Dunne, J. P., Simeon, J., Slater, R. D., Wittenberg, A. T., and Held, I. M.: Climate variability and radiocarbon in the CM2Mc earth system model, Journal of Climate, 24, 4230–4254, https://doi.org/10.1175/2011JCLI3919.1, 2011.

Jung, M., Reichstein, M., Margolis, H. A., Cescatti, A., Richardson, A. D., Arain, M. A., Arneth, A., Bernhofer, C., Bonal, D., Chen, J., Gianelle, D., Gobron, N., Kiely, G., Kutsch, W., Lasslop, G., Law, B. E., Lindroth, A., Merbold, L., Montagnani, L., Moors, E. J., Papale, D., Sottocornola, M., Vaccari, F., and Williams, C.: Global patterns of land-atmosphere fluxes of carbon dioxide, latent heat, and sensible heat derived from eddy covariance, satellite, and meteorological observations, Journal of Geophysical Research: Biogeosciences, 116, https://doi.org/10.1029/2010JG001566, 2011.

Tamocai, C., Canadell, J. G., Schuur, E. A., Kuhry, P., Mazhitova, G., and Zimov, S.: Soil organic carbon pools in the northern circumpolar permafrost region, Global Biogeochemical Cycles, 23, https://doi.org/10.1029/2008GB003327, 2009.

Taylor, K. E., Stouffer, R. J., and Meehl, G. A.: An overview of CMIP5 and the experiment design, https://doi.org/10.1175/BAMS-D-11-00094.1, 2012.